A New Millimeter-Wave Printed Dipole Phased Array Antenna Using Microstrip-Fed Coplanar Stripline Tee Junctions

Young-Ho Suh, *Member, IEEE,* and Kai Chang, *Fellow, IEEE*

Abstract—A new millimeter-wave printed twin dipole phased array antenna is developed at *Ka* band using a new microstrip-fed CPS Tee junction, which does not require any bonding wires, air bridges, or via holes. The phased array used a piezoelectric transducer (PET) controlled tunable multitransmission line phase shifter to accomplish a progressive phase shift. A progressive phase shift of 88.8° is achieved with the 5 mm of perturber length when the PET has full deflection. Measured return loss of the twin dipole antenna is better than 10 dB from 29.5 to 30.35 GHz. Measured return loss of better than 15 dB is achieved from 30 to 31.5 GHz for a 1 × 8 phased array. The phased array antenna has a measured antenna gain of 14.4 dBi with 42° beam scanning and has more than 11 dB side lobe suppression across the scan.

Index Terms—Coplanar stripline (CPS), CPS Tee junction, coplanar transmission lines, dipole antenna, microstrip-to-CPS transition, phase shifter, phased array antenna, piezoelectric transducer phase shifter, twin dipole antenna.

I. INTRODUCTION

PHASED array antenna systems usually associated with large and complex active device networks for phase shifters, which occupies large portion of the system expenses. Phased array used in military radar system requires low profile for invisibility against opponents. It also needs to be light weight especially in the applications of satellite communications. Correspondingly, the demands for low cost, low profile, small size, light weight, and less complicated phased array antenna systems are increasing nowadays for both commercial and military applications.

A printed dipole antenna satisfies the benefits of low profile, light weight, low cost and compact size, which is suitable for building phased arrays if proper phase shifters are provided. To construct a printed dipole array, several configurations have been proposed. Nesic *et al.* [1] reported a one-dimensional printed dipole antenna array fed by microstrip at 5.2 GHz. Scott [2] introduced a microstrip-fed printed dipole array using a microstrip-to-coplanar stripline (CPS) balun. In [1] and [2], the balun designs were not easy to match the impedance and the structures were too big and complicated to build an
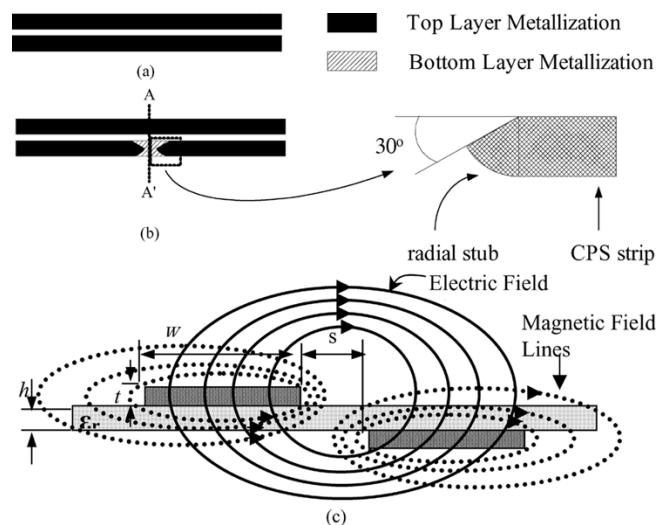
Fig. 1. CCPS structure (a) original CPS, (b) CCPS, (c) cross-sectional view at A-A' with fields distributions of the CCPS for different layers of metallization.

array. In 1998, a wideband microstrip-fed twin dipole antenna was introduced with double-sided structure operating at the frequency range from 0.61 to 0.96 GHz [3]. Zhu and Wu [4] developed a 3.5 GHz twin dipole antenna fed by a hybrid finite ground coplanar waveguide (FGCPW)/CPS Tee junction. An *X*-band monolithic integrated twin dipole antenna mixer was reported in [5] with devices directly integrated into the antenna, so no feeding network was necessary.

In this paper, a new planar printed dipole phased array antenna using a tunable phase shifter controlled by PET is presented at 30 GHz. The phased array antenna uses a new twin dipole antenna excited by a microstrip-fed CPS Tee junction [8]. The piezoelectric transducer (PET) controlled phase shifter does not require any solid-state devices and their associated driving circuits. The 1 × 8 twin dipole phased array antenna has compact size, low loss, low cost, light weight and reduced complexity as well as good beam scanning with low side lobe levels.

The PET controlled phase shifter was adopted for the low cost phased array antenna systems for the first time in [6] and [7]. In this structure, a dielectric perturber controlled by PET is used to introduce a progressive phase shift. The deflection takes place at the PET when the proper voltages are applied. Using this property of the PET, a dielectric perturber can have upward and downward movement according to the applied voltages. Consequently, if a transmission line is perturbed by a PET actuated dielectric perturber, its propagation constant
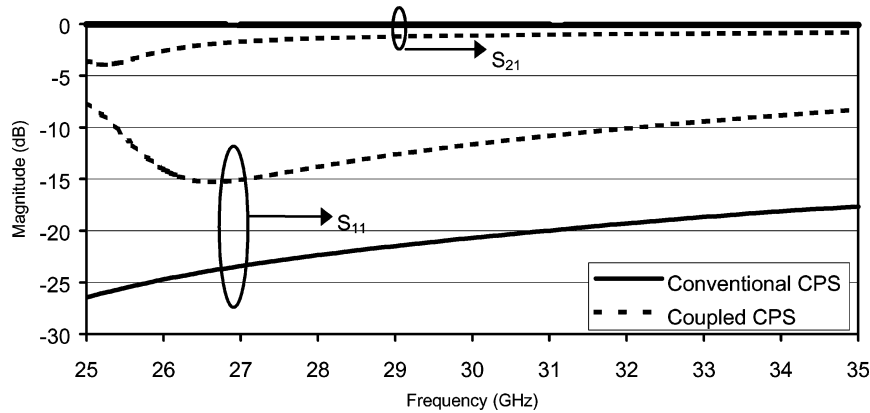
Fig. 2.   Simulated performances comparison at *Ka* band between conventional and coupled CPS.

will be changed. This phenomenon induces a variable phase shift along the transmission line controlled by PET. In [6] and [7], an end-fire Vivaldi antenna was used for covering a wide bandwidth, and a transition was required to feed antennas. Consequently, the system was large and bulky.

The new printed twin dipole phased array using a microstrip-fed CPS combined with a PET phase shifter provides low-cost, low-loss, low-profile, compact-size and low-complexity with simple antenna feeding.

II. A MICROSTRIP-FED CPS TEE JUNCTION

The twin dipole antenna is fed by a CPS. Since conventional planar transmission line is microstrip line, a microstrip-to-CPS transition is needed to feed the dipole. A microstrip-fed CPS Tee junction without using bonding wires or air bridges was introduced in [8]. In [8], the operating frequency is centered near 3.5 GHz with 0.7 dB insertion loss ranged from 2 to 4.15 GHz. The Tee junction utilized novel coupled CPS (CCPS). This transmission line can have a physical discontinuity while fields are continuous over the whole transmission line using CCPS.

The structure of original CPS and CCPS at 30 GHz is shown in Fig. 1(a) and (b). For the CPS, CCPS, Tee junction and antenna design, IE3D software [9], which uses the method of moments, is employed for full wave electromagnetic simulation. A 31 mil RT/Duroid 5870 substrate with a dielectric constant of 2.33 is used for the antenna and feeding network fabrication.

The width (W) of CPS strip is 0.65 mm and gap (s) between the strips is 0.5 mm, which has the characteristic impedance of 202 Ω. This impedance is chosen to match a dipole antenna input impedance which will be shown later. As shown in Fig. 1(b), one of the CPS strips is discontinued and is terminated with radial stubs with a rotation angle of 30° and a radius of 0.65 mm for coupling to the bottom layer metallization. The bottom layer metallization, which is coupled from the top layer's radial stubs, works as a CPS strip shown in Fig. 1(c). The radial stub is used to accomplish the smooth field transition. The wideband coupling performance of radial stubs has been reported in the microstrip-to CPS-to-microstrip back-to-back transition for lower frequency operation [10]. The back-to-back transition has a measured 3 dB insertion loss over a frequency range from 1.3 to 13.3 GHz (1:10.2) and return loss

is better than 10 dB. The radial stub provides virtual short to the bottom layer metallization, which depends on the radius of the radial stub. Hence, smaller radius of radial stub gives higher operating frequency with minimal insertion loss and return loss deteriorations compared to the original CPS configuration.

Performances of CCPS are simulated with IE3D and compared with those of conventional CPS as shown in Fig. 2. The simulated transmission line length is about 5 mm and the conventional CPS has almost zero insertion loss with that short length transmission line. Fig. 2 shows that the insertion loss of CCPS is deteriorated by about 1 dB as compared with that of conventional CPS for the frequency range from 29.2 GHz to 35 GHz and the return loss is better than 10 dB. Insertion loss deterioration of less than 2 dB covers the wider frequency range from 26.4 GHz to 35 GHz. From the above results, CCPS shows that fields are continuous all over the transmission line with the aid of radial stub, though a discontinuity is introduced at one of the CPS strips.

The structure of microstrip-fed CPS Tee junction at 30 GHz is shown in Fig. 3. The Tee junction has the characteristic impedance of 202 Ω at each output port 1 and 2. The input impedance to the microstrip feed at port 3 is about 101 Ω, which is half of 202 Ω. Radial stubs effectively rotate the electric fields from parallel to the normal to the substrate to have a good coupling to the bottom metallization, which provides the ground of microstrip line.

The Tee junction is simulated with IE3D to verify the performance at 30 GHz. Simulated performance of the Tee junction is shown in Fig. 4. The simulated performance shows that the Tee junction equally splits the power to each CPS port with 1.2 dB insertion loss at 30 GHz. Simulated 2 dB insertion loss bandwidth of the Tee junction is from 27.2 to 34.8 GHz, and the return loss is better than 20 dB. Because of high frequency operation bandwidth restriction of the microstrip-to-CPS transition in [8], the Tee junction is not measured but simulation results quite verifies its performances.

III. TWIN DIPOLE ANTENNA USING MICROSTRIP-FED CPS TEE JUNCTION

The structure of the twin dipole antenna is illustrated in Fig. 5. The twin dipole antenna utilizes the microstrip-fed CPS
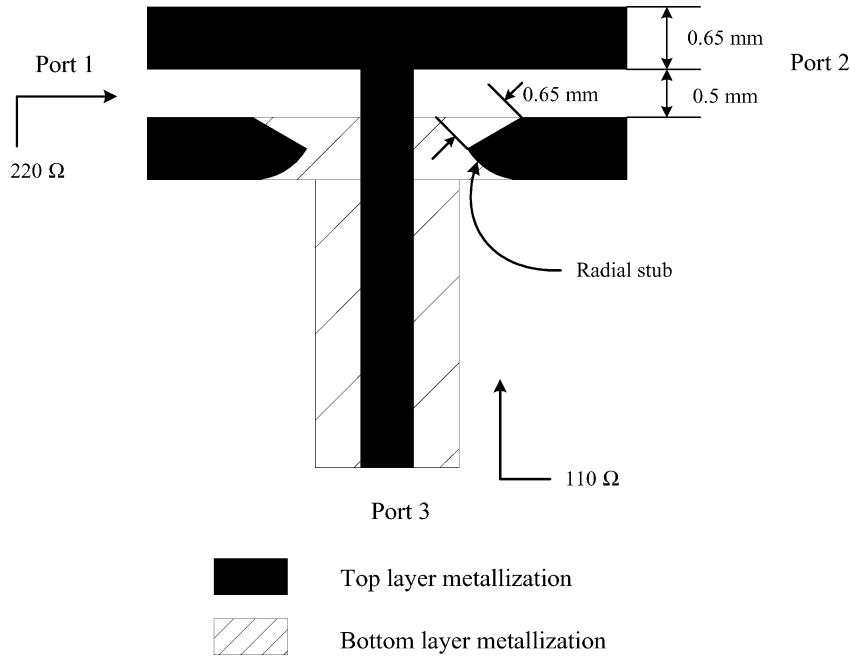
Fig. 3.   Structure of *Ka*-band microstrip-fed CPS Tee junction for twin dipole antenna feeding near 30 GHz.
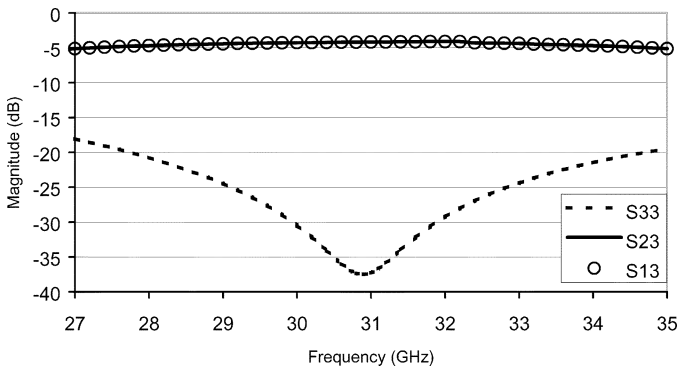

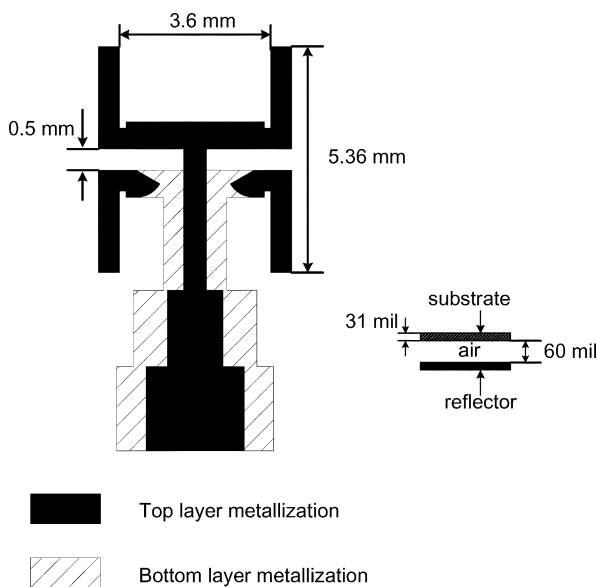Fig. 4.   Simulated performance of the Tee junction near 30 GHz.

Fig. 5.   Structure of printed twin dipole antenna using a microstrip-fed CPS Tee junction.

Tee junction as discussed in Section II. The antenna is placed in front of a reflector for uni-directional radiation. The reflector is spaced from the antenna at the distance of 1.5 mm (60 mil), which is about 0.15 λ_0. The length of dipole is 5.3 mm or 0.53 λ_0. The spacing between dipoles was optimized to be 0.36 λ_0 because of an insertion loss increase in CCPS in the Tee-junction with a long coupled line such as 0.5 λ_0, causing a gain drop. Mutual coupling normally takes place when antenna spacing is less than a half wavelength. Twin dipole antenna's input impedance is supposed to have some reactance due to this coupling effect. By adjusting the reflector's spacing, this reactance can be minimized with a small change in input impedance.

The input impedance of a single dipole antenna is around 202 Ω. The strip width (W) and gap (s) between strips of CCPS at the CPS Tee junction in Section II are determined to have a CCPS characteristic impedance identical to the dipole antenna input impedance for good impedance matching.

Measured return loss of the twin dipole antenna is better than 10 dB from 29.5 to 30.35 GHz as shown in Fig. 6. Measured and simulated return losses have good agreements. For measurements, a quarter-wavelength transformer with limited bandwidth is used and causes small discrepancies between simulated data and measurements. Radiation patterns of the antenna are measured in an anechoic chamber. The measured radiation patterns are shown in Fig. 7. E and H-plane radiation patterns are quite similar to each other for the twin dipole antenna as discussed in [4]. Measured E and H-plane gains are about 7.6 and 7.7 dBi with the 3 dB beamwidths of 32° and 34°, respectively. The measured cross-polarizations at broadside are about 47.7 and 42.4 dB down compared with the copolarization levels in E and H-plane, respectively. Gains and 3 dB beam widths of E and H-planes are quite close to each other. Some discrepancies of gains and 3 dB beam widths are partly due to the small misalignments of the antenna in millimeter-wave frequencies.
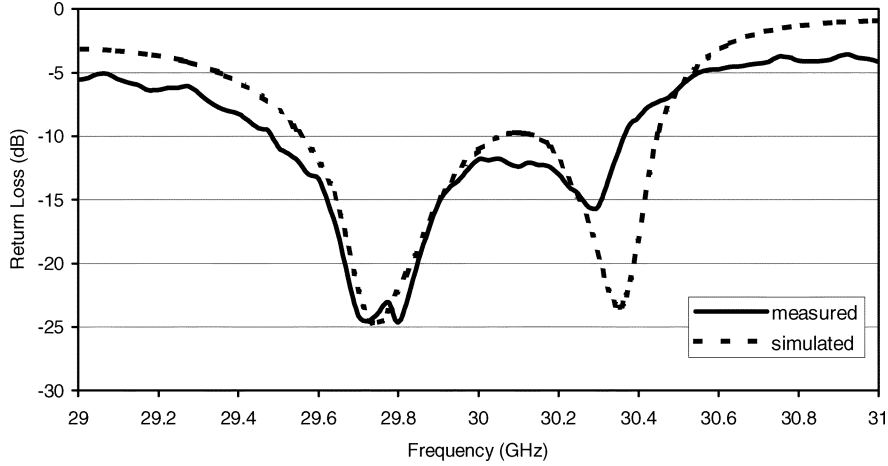
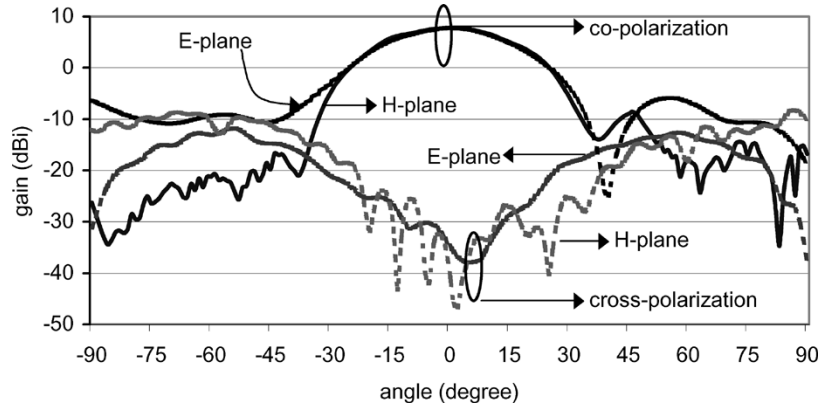Fig. 6.   Simulated and measured return loss of the twin dipole antenna.

Fig. 7.   Measured radiation patterns of the twin dipole antenna.

IV. PHASED ARRAY ANTENNA WITH MULTITRANSMISSION LINE PET CONTROLLED PHASE SHIFTER

For the linear phased array, an array factor is a function of the progressive phase shift Φ and the element spacing d. The array factor is given as

$$AF = \sum_{n=1}^{N} e^{j(n-1)\Psi} \qquad (1)$$

where

$$\Psi = k_0 d \cos \theta_0 + \Phi. \qquad (2)$$

where k_0 is expressed as $2\pi/\lambda_0$ and θ_0 is beam scanning angle. N is the number of elements.

The progressive phase shift causes the radiation emitted from the array to have a constant phase front that is pointing at the angle θ_0. This beam scanning angle (θ_0) is also a function of Φ and d, given by

$$\theta_0 = \sin^{-1}\left(\frac{\Phi}{k_0 d}\right) = \sin^{-1}\left(\frac{\Phi \lambda_0}{2\pi d}\right). \qquad (3)$$

The array factor in (1) can also be expressed as (4) below in an alternate, compact and closed form whose function and their distributions are more recognizable [11]. It is assumed that the reference point is the physical center of the array.

$$AF \cong \left[\frac{\sin\left(\frac{N}{2}\Psi\right)}{\frac{\Psi}{2}}\right]. \qquad (4)$$

The total field of array is equal to the field of a single element positioned at the origin multiplied by an array factor, which is expressed as

$$\overline{E}_{\text{total}} = \left[\overline{E}_{\text{single element at reference point}}\right] \times [AF]. \qquad (5)$$

From (4), the maximum value of array factor is N [11]. Hence maximum achievable gain of the array can be found from (4) and (5), which is expressed as

$$\begin{aligned}
\text{Gain}_{\max}(\text{dB}) &= \text{Gain}_{\text{single element}}(\text{dB}) + AF_{\max}(\text{dB}) \\
&= \text{Gain}_{\text{single element}}(\text{dB}) + 10\log_{10} N(\text{dB}).
\end{aligned} \qquad (6)$$

In (6), the effect of mutual coupling between elements is excluded for the simplicity. Mutual coupling normally degrades arrayed antenna gain. Equation (6) can be used for the gain approximation of the array. To achieve more accurate calculation including mutual coupling effects, a full-wave electromagnetic simulation can be used for antenna array analysis.
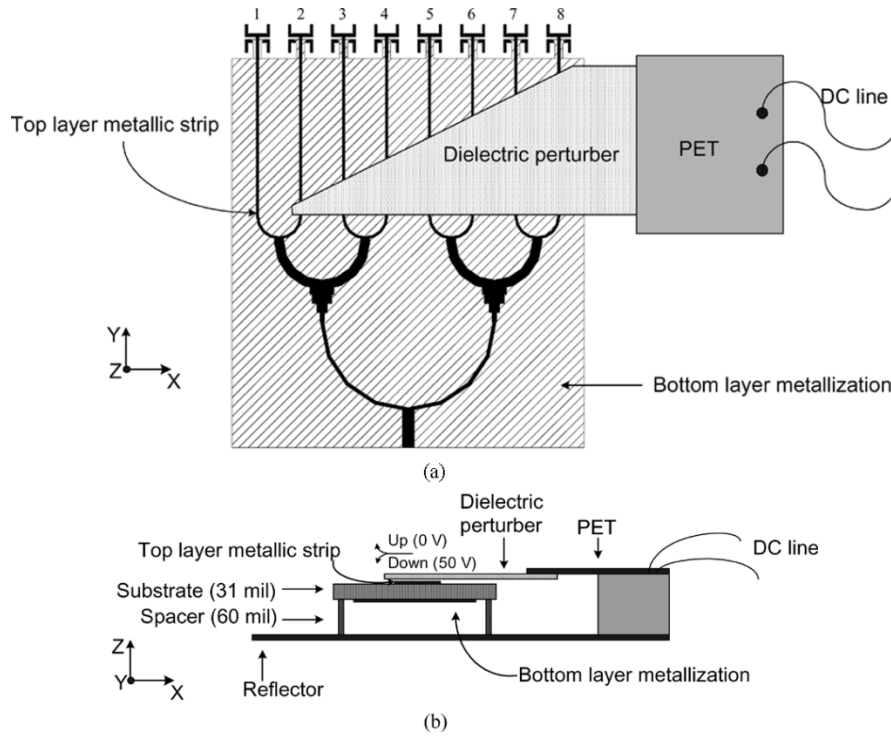
Fig. 8. Structure of printed dipole phased array antenna controlled by PET (a) top view and (b) side view.

The structure of 1×8 printed twin dipole phased array antenna is shown in Fig. 8. A conventional microstrip power divider with binominal impedance transformers is used for feeding network to cover the wide bandwidth. The bottom metallization provides good ground plane for the microstrip.

To obtain the required phase shift, the 101 Ω microstrip line, which has the same input impedance as the twin dipole antenna, is perturbed with a dielectric perturber actuated by PET. The length of dielectric perturber varies linearly from 5 to 35 mm on top of line 2 to line 8 in Fig. 8. The first line is not perturbed. The PET is configured to have no deflection (no perturbation) when a DC voltage of 0 V is applied, and full deflection (full perturbation) when a DC voltage of 50 V is applied. A 50 mil RT/duroid 6010.2 with a dielectric constant of 10.2 is used as the dielectric perturber.

The amount of phase shift is linearly proportional to the length of perturber [7], which is expressed as

$$\Delta\Phi_n = L_{\text{perturber},n} \bullet \Delta\beta_n \quad (7)$$

where, $L_{\text{perturber},n}$ is the perturber length along the nth transmission line. $\Delta\beta_n$ represents the differential propagation constant expressed as

$$\Delta\beta_n = \beta_{\text{unperturbed}} - \beta_{\text{perturbed},n} \quad (8)$$

where $\beta_{\text{perturbed},n}$ represents the propagation constant of the nth perturbed transmission line, which is microstrip in this case. Since the first perturbed microstrip line (i.e., the second line or line 2) has the minimum perturbed length, the following relationship is obtained.
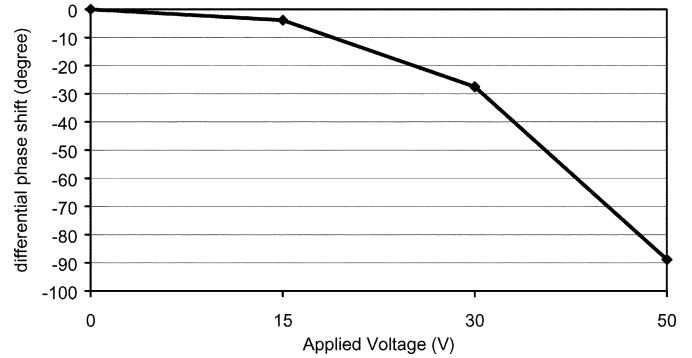
$$\Delta\Phi_2 = \Phi. \quad (9)$$

Fig. 9. Differential phase shift for 5 mm dielectric perturber controlled by PET.

With a dielectric perturber of 5 mm, Fig. 9 shows that a differential phase shift of 88.8° takes place with a 2 dB insertion loss. Narrower microstrip line generates larger phase shift but the insertion loss is increased. Hence, a proper microstrip line's width should be chosen for having a good phase shift as well as low insertion loss.

Table I summarizes the design and measured parameters for the twin dipole phased array. The parameter values in Table I are useful in analytical calculations of the scanning angle (θ_0), maximally achievable gain, and optimum element spacing (d) of the phased array.

According to (7) and (8), the perturber's length can be determined for a desired phase shift. A length of 5 mm dielectric perturber produces about 88.8° differential phase shift. Accordingly, the length of each neighboring perturbed line is increased by 5 mm. The length of perturber for the final microstrip ($L_{\text{perturber,8th}}$) is about 35 mm, which gives a differential phase shift of 621.6°.

TABLE I
PARAMETER VALUES OF THE TWIN DIPOLE PHASED ARRAY

Frequency (GHz)	Measured single element gain (dBi)	Measured progressive phase shift (Φ)	Spacing between elements (d)	Number of elements (N)
30	7.7	88.8°	6.7 mm	8

TABLE II
COMPARISON AMONG ANALYTICAL, SIMULATION, AND MEASURED RESULTS OF THE 1 × 8 PHASED ARRAY

	Beam scanning (θ_0)	Unperturbed gain (dBi)	Element spacing (d)
Analytical calculation	± 19.47°	16.73	7.5 mm
IE3D simulation	± 20°	16.48	7.4 mm
Measured	-20° ~ + 22°	14.4	7.4 mm

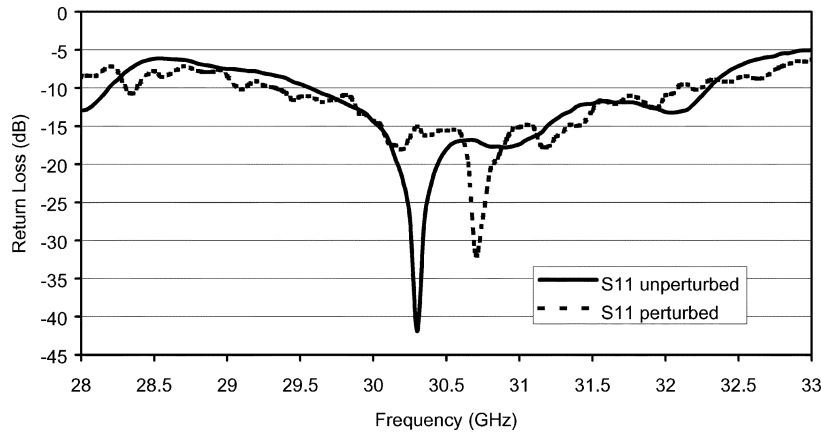Fig. 10.   Measured return loss of the printed twin dipole phased array antenna.

IE3D analysis shows that a progressive phase shift of 88.8° gives around ±20° beam scanning with low side lobe levels. An analytical scan angle can also be obtained using (3), and maximally achievable gain of the phased array can be obtained from (6). The maximum spacing (d) between elements to avoid grating lobes is expressed as

$$d = \frac{\lambda_0}{1 + \sin\theta_0}. \qquad (10)$$

From analytical equations in (3), (6) and (10) and the parameters in Table I, the calculated θ_0, maximally achievable gain, and maximum spacing d are calculated to be 19.47°, 16.73 dBi, and 7.5 mm, respectively. The results agree very well with IE3D simulation as given in Table II.

Measured return loss of the 1 × 8 twin dipole array is plotted in Fig. 10. The measured return loss is about 41.9 dB at 30.3 GHz for the unperturbed twin dipole phased array antenna. With perturbation by the dielectric perturber, the return loss is about 31.8 dB at 30.7 GHz, which shows a 0.4 GHz frequency shift compared with the unperturbed result. For a bandwidth from 30 to 31.5 GHz, a measured return loss is better than 15 dB.

V. PHASED ARRAY MEASUREMENTS

The phased array is measured in an anechoic chamber. As shown in Fig. 8, the antenna is arrayed for the H-plane beam scanning. To accomplish bidirectional beam scanning, two triangular perturbers are used side by side [12]. PET actuation for the dielectric perturber is configured as 0 V for no perturbation (no PET deflection) and 50 V for full perturbation (full PET deflection). The measured twin dipole phased array antenna gain without perturbation (0 V for PET) is about 14.4 dBi with a 3 dB beam width of 6° as shown in Fig. 11. The fully perturbed antenna with a dielectric perturber controlled by PET shows about 42° (−20° ~ +22°) beam scanning with the gain of 12.2 dBi. Side lobe levels of the steered beam are more than 11 dB down compared with main beam. The gains of steered beams are about 2.2 dB down due to the insertion loss incurred by dielectric perturbation. The beam can be dynamically steered depending on the voltages applied to PET because the amount of phase shift changes according to the applied voltages on PET as shown in Fig. 9.

The comparison among analytical, simulation, and measured results of the phased array are exhibited in Table II. Beam scanning angle is following closely among analytical, IE3D simula-
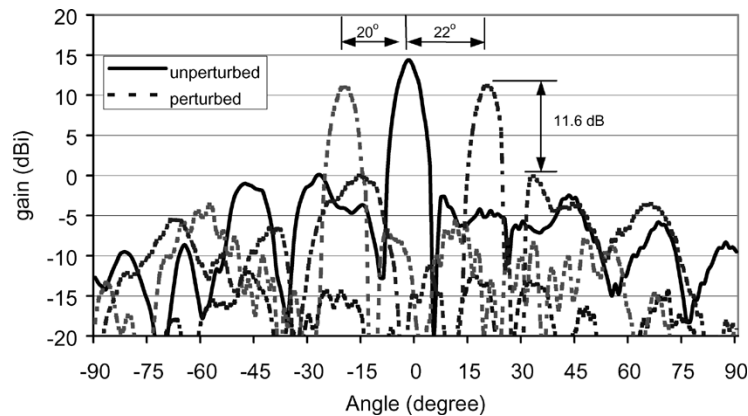
Fig. 11. Measured H-plane radiation pattern for twin dipole phased array antenna at 30 GHz. Measured beam scanning is from $-20°$ to $+22°$ with full perturbation.

tion, and measured results. Measured unperturbed gain is about 2.3 dB lower than analytical or IE3D simulated data. This is due to the insertion loss of power divider and the mutual coupling effects among elements, which normally degrades antenna gain. The measured gains of steered beams are about 2.2 dB down compared to that of unperturbed beam due to the insertion loss incurred by dielectric perturbation.

VI. CONCLUSION

A new printed twin dipole phased array antenna is developed at 30 GHz using a multitransmission line tunable phase shifter controlled by a PET. The new twin dipole antenna is designed using a microstrip-fed CPS Tee junction. To construct the Tee junction, CCPS is used to have a physical discontinuity at CPS while fields are continuous all over the transmission line. The Tee junction effectively splits power to each CPS output port with low insertion loss. The PET actuated phase shifter requires only one (one-directional beam scanning) or two (bi-directional beam scanning) applied voltages to produce the progressive phase shift. A PET controlled phase shifter is tested and optimized for the proper phase shift with minimal insertion loss. The twin dipole phased array antenna shows a $42°$ ($-20° \sim +22°$) beam scanning with more than 11 dB side lobe suppression across the scan. The phased array should find many applications in wireless communications and radar systems.

ACKNOWLEDGMENT

REFERENCES

[1] A. Nesic, S. Jovanovic, and V. Brankovic, "Design of printed dipoles near the third resonance," in *Proc. IEEE Int. Antennas and Propagation Symp. Dig.*, vol. 2, Atlanta, GA, 1998, pp. 928–931.

[2] M. Scott, "A printed dipole for wide-scanning array application," in *Proc. IEEE 11th Int. Conf. Antennas and Propagation*, vol. 1, 2001, pp. 37–40.

[3] G. A. Evtioushkine, J. W. Kim, and K. S. Han, "Very wideband printed dipole antenna array," *Electron. Lett.*, vol. 34, no. 24, pp. 2292–2293, Nov. 1998.

[4] L. Zhu and K. Wu, "Model-based characterization of CPS-fed printed dipole for innovative design of uniplanar integrated antenna," *IEEE Microwave and Guided Wave Lett.*, vol. 9, pp. 342–344, Sept. 1999.

[5] K. L. Deng, C. C. Meng, S. S. Lu, H. D. Lee, and H. Wang, "A fully monolithic twin dipole antenna mixer on a GaAs substrate," in *Proc. Asia Pacific Microwave Conf. Dig.*, Sydney, NSW, Australia, 2000, pp. 54–57.

[6] T. Y. Yun and K. Chang, "A phased-array antenna using a multi-line phase shifter controlled by a piezoelectric transducer," in *IEEE Int. Microwave Symp. Dig.*, vol. 2, Boston, MA, 2000, pp. 831–833.

[7] ——, "A low-cost 8 to 26.5 GHz phased array antenna using a piezoelectric transducer controlled phase shifter," *IEEE Trans. Antennas Propagat.*, vol. 49, pp. 1290–1298, Sept. 2001.

[8] Y. H. Suh and K. Chang, "A microstrip fed coplanar stripline Tee junction using coupled coplanar stripline," in *Proc. IEEE Int. Microwave Symp. Dig.*, vol. 2, Phoenix, AZ, 2001, pp. 611–614.

[9] *IE3D*, 8.1 ed., Zeland Software Inc., 2001.

[10] Y. H. Suh and K. Chang, "A wideband coplanar stripline to microstrip transition," *IEEE Microwave and Wireless Components Lett.*, vol. 11, pp. 28–29, Jan. 2001.

[11] C. A. Balanis, *Antenna Theory Analysis and Design*, 2nd ed. New York: Wiley.

[12] T. Y. Yun, C. Wang, P. Zepeda, C. T. Rodenbeck, M. R. Coutant, M. Y. Li, and K. Chang, "A 10- to 21-GHz, low-cost, multifrequency, and full-duplex phased-array antenna system," *IEEE Trans. Antennas Propagat.*, vol. 50, pp. 641–650, May 2002.

Young-Ho Suh (S'01–M'02) received the B.S degree in electrical and control engineering from Hong-Ik University, Seoul, Korea, in 1992, and the M.S and Ph.D. degrees in electrical engineering from Texas A&M University, College Station, TX, in 1998, and 2002, respectively.

From 1992 to 1996, he worked for LG-Honeywell Co. Ltd., Seoul, Korea, as a Research Engineer. From 1996 to 1998, he worked on developing robust wireless communication systems for GSM receiver under multipath fading channel for his M.S degree. From 1998 to 2002, he was a Research Assistant in the Electromagnetics and Microwave Laboratory, Department of Electrical Engineering, Texas A&M University, College Station, TX, where he was involved in rectenna design for wireless power transmissions, phased array antennas, and coplanar transmission line circuit components development. In May 2002, he joined Mimix Broadband Inc., Houston, TX, as a Senior Microwave Design Engineer, where he is working on state-of-the-art microwave/millimeter-wave active circuit designs including low noise/power amplifiers, receivers, transmitters, and transceiver modules for LMDS, point-to-point, point-to-multipoint radio systems in *Ka* band using GaAs MMICs. His research area includes state-of-the-art millimeter-wave transceiver modules, transitions between dissimilar transmission lines, uniplanar transmission line analysis and components development, microwave power transmission, antennas for wireless communications, and phased array antennas.

Kai Chang (S'75–M'76–SM'85–F'91) received the B.S.E.E. degree from the National Taiwan University, Taipei, Taiwan, R.O.C., the M.S. degree from the State University of New York at Stony Brook, and the Ph.D. degree from the University of Michigan, Ann Arbor, in 1970, 1972, and 1976, respectively.

From 1972 to 1976, he worked for the Microwave Solid-State Circuits Group, Cooley Electronics Laboratory, University of Michigan, as a Research Assistant. From 1976 to 1978, he was employed by Shared Applications, Inc., Ann Arbor, where he worked in computer simulation of microwave circuits and microwave tubes. From 1978 to 1981, he worked for the Electron Dynamics Division, Hughes Aircraft Company, Torrance, CA, where he was involved in the research and development of millimeter-wave solid-state devices and circuits, power combiners, oscillators and transmitters. From 1981 to 1985, he worked for the TRW Electronics and Defense, Redondo Beach, CA, as a Section Head, developing state-of-the-art millimeter-wave integrated circuits and subsystems including mixers, VCOs, transmitters, amplifiers, modulators, upconverters, switches, multipliers, receivers, and transceivers. He joined the Electrical Engineering Department of Texas A&M University in August 1985 as an Associate Professor and was promoted to a Professor in 1988. In January 1990, he was appointed E-Systems Endowed Professor of Electrical Engineering. He authored and coauthored several books "*Microwave Solid-State Circuits and Applications*" (New York: Wiley, 1994), "*Microwave Ring Circuits and Antennas*" (New York: Wiley, 1996), "*Integrated Active Antennas and Spatial Power Combining*" (New York: Wiley, 1996), and "*RF and Microwave Wireless Systems*" (New York: Wiley, 2000). He served as the editor of the four-volume "*Handbook of Microwave and Optical Components*" (New York: Wiley, 1989 and 1990). He is the Editor of the *Microwave and Optical Technology Letters* and the *Wiley Book Series in Microwave and Optical Engineering*. He has published over 350 technical papers and several book chapters in the areas of microwave and millimeter-wave devices, circuits, and antennas. His current interests are in microwave and millimeter-wave devices and circuits, microwave integrated circuits, integrated antennas, wideband and active antennas, phased arrays, microwave power transmission, and microwave optical interactions.

Dr. Chang received the Special Achievement Award from TRW in 1984, the Halliburton Professor Award in 1988, the Distinguished Teaching Award in 1989, the Distinguished Research Award in 1992, and the TEES Fellow Award in 1996 from the Texas A&M University.